Attenuation Relations for Peak Horizontal and Vertical Accelerations of Earthquake Ground Motion in Iran: A Preliminary Analysis

Ali A. Nowroozi

Department of Ocean, Earth and Atmospheric Science, Old Dominion University, Norfolk, Virginia, 23528, email: anowrooz@odu.edu

ABSTRACT: *Attenuation relations are developed based on information in the Iranian acceleration data bank (IADB) containing 279 entries from about 30 seismogenic areas across the country. The peak ground horizontal (PGH) and peak vertical accelerations (PGV), varies from a few cm/s² to over 1000 cm /s². Moment magnitudes (Mw) vary from about 3.0 to 7.4; and earthquake depths vary from near surface to over 100 km; however, except a majority of depth that are kept at 33 km in the locating process, most depths are about 10 km. Epicentral distances (EPD) vary from 2 km to nearly 250 km. The data bank also includes four site conditions, S. The least squared multi-stage regression solutions for acceleration attenuation are calculated for three cases. The predicted PGH and PGV accelerations are compared with uncorrected high accelerations components near the source of Bam earthquake of 2003; the high PGH acceleration is reproduced, but the estimated PGV acceleration is lower by a factor of 2 to 3. In addition, estimations based in this work are compared with several other studies and discrepancies are discussed.*

Keywords: Attenuation relations; Vector sum; Horizontal and vertical components of acceleration; Iran

1. Introduction

Iran has high degree of seismic activity. Nowroozi [1] and Nowroozi and Ahmadi [2] based on Nowroozi [3] concept on seismotectonic provinces of Iran reported high accelerations for many parts of the country. They estimated that in a time exposure of about 300 years nearly the entire country would experience an acceleration of 0.5g except in a few narrow areas along north-west south-east trends. For example Esfahan-Sirjan provinces will experience 0.24*g*.

Earthquakes with magnitude 6 may occur in Fars, High Zagros and Foothill Folded Series seismotectonic provinces in 4, 7 and 11 year intervals [1], and magnitude 7 earthquakes may occur in Fars Folded Series, Alborz, Kopet-Dagh and central Iran seismotectonic provinces in nearly every 50 years. Human toll and cost to national economy is very large and unacceptable.

There are many reasons for this extensive death toll. The most important factors include: Deficiency of public education in earthquake risk and seismology and earthquake resistant constructions. Public is not aware of advantages in living in the houses designed to resist earthquakes, although it may cost more. Design of buildings by engineers without sufficient training in structural dynamics and earthquake resistant designs, undergraduate engineering curriculums that do not include courses in earthquake resistant design, foundation engineering, soil mechanics and quaternary geology, historic nature and existence of adobe buildings in many rural areas and large cities, even in the capital city Tehran are additional problems. Finally, lack of enforcing the existing seismic codes, poor construction technique, construction materials and supervision, unsuitable geological locations for

many villages in the rural area and even big cities also are other contributing factors.

These issues, together with high seismicity rate and lack of a short term response (in order of hours) shortage of trained sniffing dogs to find live buried persons and lack of accessible roads to provide help, have produced over 150,000 human toll during the past century. The Tabas earthquake of 1978, Manjil earthquake of 1990 and Bam earthquake of 2003 have caused nearly 100,000 dead [4]. The number of injured, orphans and homeless may be even higher.

Estimation of horizontal and vertical components of acceleration from the seismic sources that may produce a certain magnitude is critical for design of structures to resist earthquakes. Acceleration attenuation relations for a given magnitude are essential for construction of safe houses and other public edifices, complex industrial structures that are essential for economical well being of the nation, and the safety of the Iranian people and their national security. For example refineries, ports, factories, power stations, bridges, roads, hospitals, schools, universities and many others facilities can be made safer by estimating the probable accelerations at their sites and retrofit the facilities to be safe at higher acceleration. In addition, acceleration attenuation relations may be used in calculations for seismic mitigation, and deterministic and probabilistic approaches to seismic risk and hazard analysis. Decaninni and Mollaiolli [5] showed that this engineering approach is based on the analysis of the strong motion databases collected by the existing strong motion networks. These databases should contain similar source, path and site effects.

In the last few decades, the government of Iran has installed over 1000 strong motion instruments across the country for recording the ground accelerations following earthquakes [6]. Since early 2004, *BHRC* has released the most recent strong motion data of Iran on its web site (www.bhrc.ac.ir). This web site delivers the update information on the installed instruments and planned stations. So far there are no general agreements for attenuation of *PGH* and *PGV* acceleration for Iran.

In a very informative paper, Bard et al [7] published the results of 279 accelerograms (from 1974 to 1996) across Iran in the form of a table. Their table has a complete set of three components of accelerations from all accelerometers and many interpreted velocities and displacements. In addition they provide, magnitudes, depth, epicentral, macroseismic and hypo-central distances, intensities, focal mechanism solutions for some of the earthquake sources, site conditions, and other useful information for many of the records. Zare [8] and Zare et al [9] have used this data set and produced attenuation laws for central Iran, Zagros and Alborz region and entire Iran. Their equations do not include a saturation term, thus, their equations produce high value of acceleration at small epicentral distances. In this paper a saturation term is included and results are compared. The attenuation equations presented here produce a reasonable acceleration even at near source region with $EPD = 1km$ for a major earthquake; in addition it is consistent with the seismic scaling law [10,11], and accelerations saturate at near source region.

Accelerations recorded by some individual earthquakes such as Tabas, 1978, Manjil 1990, Ghir 1988, Golbaft, 1982, Sirch 1981 and Naghan 1977 are studied by some authors [12-20]. Among these, Niazi and Bozorgnia [16] presented an attenuation relation only for the Manjil event with $Ms = 7.7$, and Zare [20] presented equations for maximum horizontal ground acceleration for Manjil, Tabas, Sirch, Golbaft and Naghan earthquakes. Zare's equations have a novelty, as he has introduced a term related to predominant period. This parameter can be estimated from a graph of predominant periods versus epicentral distances. In addition, Campbell and Bozorgnia [21,24] have used the acceleration from Tabas and Manjil earthquakes together with a large number of acceleration records across the world for their study of near source attenuation of *PGH* and *PGV* accelerations. However, Panza et al [25] has shown that *PGA* is a single value indicator widely used in the seismic hazard analysis that alone can not adequetely indicates all the effects associates with ground shaking. This is because the frequency content and the duration of a seismic wavetrain play the decisive roles.

In this paper, the goals are to present the attenuation relationships for *PGH* and *PGV* accelerations based on acceleration records in Iran as reported by Bard et al [7]. In addition, a comparison has been made between the results of this work and some of other studies for Iran and other regions. Also, based on results of this work, an attempt has been undertaken to predict the high acceleration components recorded [19] near the source of Bam earthquake of 2003 in the city of Bam.

2. Presentation and Treatment of Data

For development of attenuation relations a complete

set of accelerations, epicentral distance, depths, and magnitudes is required. The author has taken liberty to complete the gaps in the Iranian Acceleration Data Bank (*IADB*) in following manner:

1. Each magnitude scale, *ML*, *mb*, *Ms* and *Mw* had gaps. It was decided to use Moment magnitude *Mw* as an independent parameter; because nearly in all reported attenuation relations *Mw* is used as an independent parameter. The original *IADB* contains a few local magnitudes, *ML*, *Mw* and a moderate number of *MS* but a large number of body magnitudes, *mb*. Figure (1) shows the range of reported Ms magnitudes versus other magnitudes.
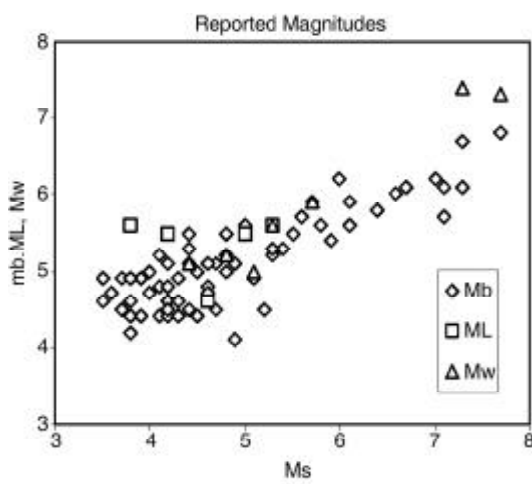

Figure 1. Reported magnitudes: Graph of Mb, ML, and MW magnitudes versus Ms magnitude.

When only local magnitude was available, the equation $mb = 1.7+0.8*ML-0.01*ML^2$ [26] was used for conversion of *ML* to *mb*. When *mb* magnitude was available and *Ms* magnitude was not available, $Ms = 1.6207*mb - 3.15$ was used for conversion. This relation is calculated from data of Bard et al [7] and has a multiple correlation coefficient of 0.8695 or a correlation coefficient of 0.932. This equation is very similar to $Ms = 1.59*mb - 3.7$ given by Richter [26]. Although body wave magnitude was not used in the analysis, for completeness, the equation for conversion of *Ms* to *mb* was presented. The body wave magnitude *mb* also may be calculated from surface wave magnitude by $mb = 0.5365*Ms+2.5061$ using the data reported in Bard et al [7]. The correlation coefficient for this equation is also 0.932 as expected. The high value of the correlation coefficients indicate that the calculated *Ms* and *mb* are consistent with the other *Ms* and *mb* magnitudes reported by Bard

et al [7].

When *Mw* was not available *Ms* was used for calculation of *Mw*. From limited *Ms* and *Mw* data in the Iranian acceleration data bank, the author dervired, $Mw =0.69*Ms + 1.92$, with a correlation coefficient of 0.983. Because of its high correlation coefficient, this equation is used to covert *Ms* to *Mw*. Only 91 earthquakes have *Ms* magnitude larger than or equal to 5. The events are listed in Appendix (1). For consistency, recalculated *Mw* is used in the final analysis.

2. For three events epicentral distances were not reported. Macroseismic distances is used to complete the gaps. The range of *EDP* is between 2 to about 250*km*. Figure (2) presents variations of calculated magnitudes with epicentral distances in *km*.
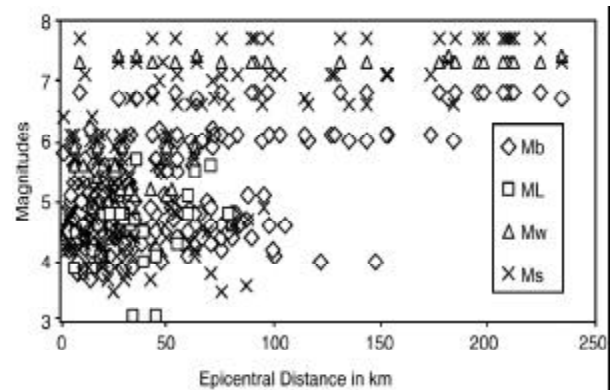

Figure 2. Magnitude distribution with epicentral distance after magnitude conversion.

3. Because acceleration is a vector quantity, the peak ground horizontal acceleration was defined *PGH*, as vector sum of the two horizontal components. For example, the reported peak ground accelerations for the Tabas 1978 earthquake are: $h1=1103$, $h2=841$, cm/s^2 respectively; thus, the vector sum is equal to $(1103^2 + 841^2)^{1/2}$ or $1387.04 cm/s^2$. This value is adopted as peak ground horizontal acceleration or *PGH* acceleration.

Some authors have used the largest value of the two horizontal components, or used the geometrical mean, or the average of recorded horizontal components of acceleration for calculation of *PGH* acceleration. The author believes that the mean methods underestimate the value of *PGH*. For example, in case of Tabas earthquake, the largest component is $1103 cm/s^2$. The average or arithmetic mean is

$972.0cm/s^2$; the geometrical mean is $963.13cm/s^2$. However, the vector method gives $1387.04cm/s^2$. It is interesting to note that both mean methods give an acceleration value, which is smaller than the largest observed value, but the result of vectorial method is higher than the largest observed value and probably closer to the actual *PGH* acceleration. This approach may be more conservative but also it is more prudent and closer to reality because structural elements in horizontal plane are under loads from both components of horizontal accelerations almost simultaneously.

Certainly, it is important for structures to resist earthquake excitation. In most cases, a priori, a design engineer is not aware of the direction of the acceleration vector. Therefore, if a critical element of structure is under load of the combined component of horizontal accelerations, safety demands that the element be designed for the load of that acceleration.

The vector sum method requires that the two horizontal components arrive at the same time, but it was not possible to establish the timing from the table of Bard et al [7]. In any case most accelerograms are hand digitized and may contain some timing errors. Hopefully new digital accelerometers will provide badly needed data in this area and provide the exact arrival time of each digital component of accelerations. Then, *PGH* acceleration may be calculated from the rotation of the coordinate system, by using the back azimuth to the earthquake source and the two horizontal components of accelerations.

4. The focal depth was not used as an independent parameter in regression process; because, there was a large number of focal depths kept at $33km$. In addition, recent research shows that some of the reported deeper earthquakes are acually shallower [22]. The major peaks are at $33km$ and $10km$, but high frequency at $33km$ is not real, as depth was kept constant at this level during earthquake location.

5. Bard et al [7] presented four different site categories. They reported 117 rock sites, 52 alluvial sites, 70 gravel and sandy sites, and 39 soft soils sites. The author believed that there were not sufficient ranges of variability of different parameters in each site category to use them separately in each analysis. Thus, three independent analyses were made. In the first analysis site conditions was not included. In a second analysis, site category 1 and 2 was combined and considered as firm rock site category. Category 3 and 4 was combined together and were called

soft soil site category. This is more in line with recent work of Campbell and Bozorgnia [24] and [27]. In the third case all site categories was considered in one analysis. The effects of site conditions on accelerations will be discussed later. However, it is indicated experimentally [28] and theoretically [29,30] that the so-called local site effects can be strongly dependent on the seismic source characteristics.

6. The source types as additional parameters was not used. The table by Bard et al [7] has this information for only a limited numbers of events, and it was not possible to complete any of the gaps.

Figure (3) presents the frequency distribution of original site conditions, depth, recalculated *Mw* magnitude, *H*1, *H*2 and vertical components of ground accelerations as a function of epicentral distances. The frequency counts are linear but the epicentral distances are given in logarithmic scale to emphasize the relative spread of the counts. Figures (4) and (5) show the range and pictorial relation of peak horizontal acceleration, *PGH*, peak vertical acceleration, *PGV*, for site condition 1, 2, 3 and 4. Figure (6) shows the *H*1, *H*2, vertical or *PGV* and *PGH* components of acceleration versus *Mw* and *EPD* for all site combined. By comparison of Figure (6) and Figures (4) and (5), it is clear that the total data are better distributed over acceleration, magnitude and distance ranges. Thus, the total data was used rather than data in each case.

There are three *PGH* accelerations larger than $1000m/s^2$. They belong to Tabas, Manjil and Naghan events. Also, there are three large *PGV* accelerations. They are $848cm/s^2$, $548cm/s^2$ and $993cm/s^2$ for the Tabas, Manjil and Ebrahimabad events respectively.

3. Attenuation Relations

Many mathematical forms of attenuation relations are reported in the literature. In a very careful work, Campbell [23] reviews the published work during 1974-1984; he also proposes steps for model selection and analysis procedure. In addition he gives a summary of 19 equations for the United States and some other areas. In a recent web site, Leonov [31] presents an additional 13 equations for the United States, Japan, India and other parts of the world. Douglas [32-34] reported more than 120 equations during past three decades for prediction of peak ground acceleration. The equations have different forms and they are based on linear natural or base 10 logarithm,
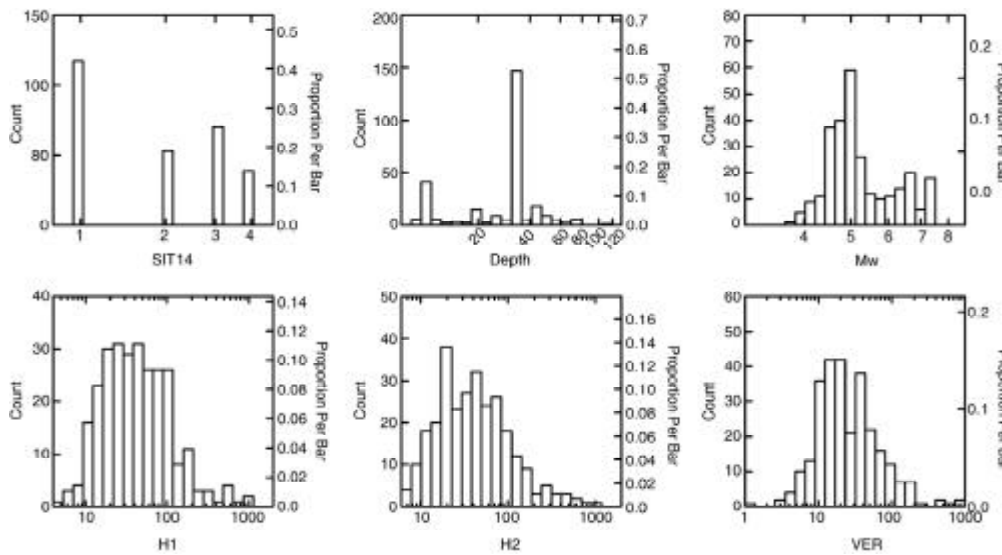
Figure 3. Frequency distribution of site parameters, S =1- 4, depth, Mw, H1, H2 and vertical components of acceleration. The x-axis is in logarithmic scale to emphasize the shape of distribution.

Figure 4. A three-dimensional view of peak ground horizontal acceleration, PGH, with epicentral distance EPD and Mw for each site condition. Site conditions are: 1 for rock sites; 2 for thin soft alluvial sites; 3 for sandy gravel sites and 4 for soft soil sites.

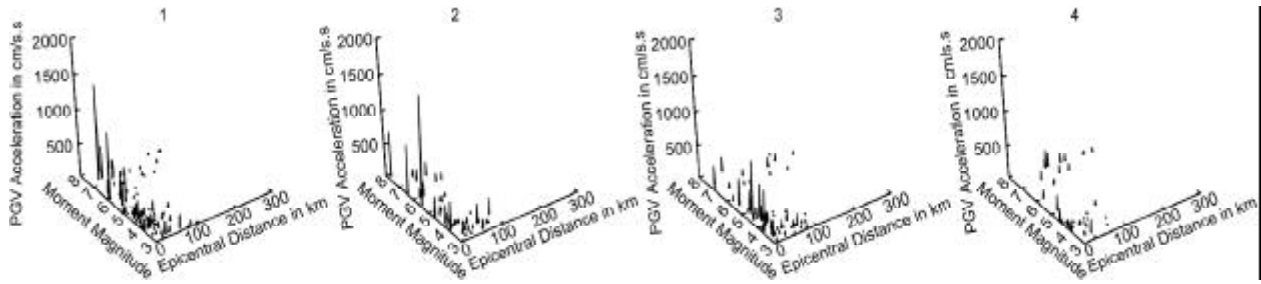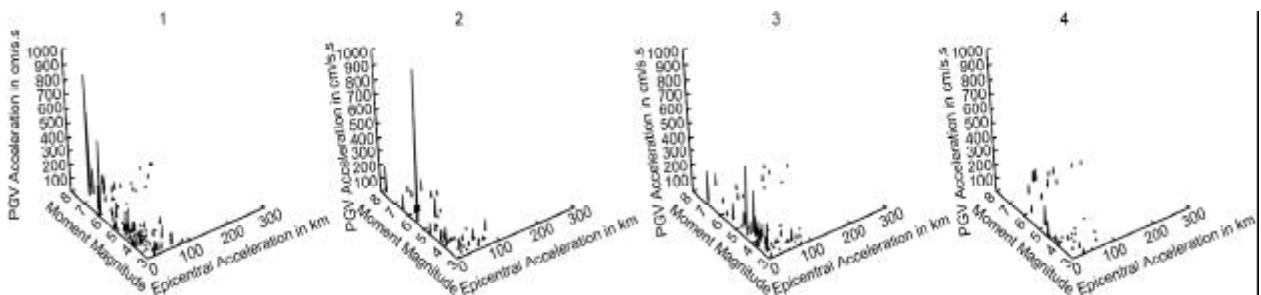**Figure 5.** A three-dimensional view of peak ground vertical acceleration, PGV, with epicentral distance EPD and Mw for each site condition.
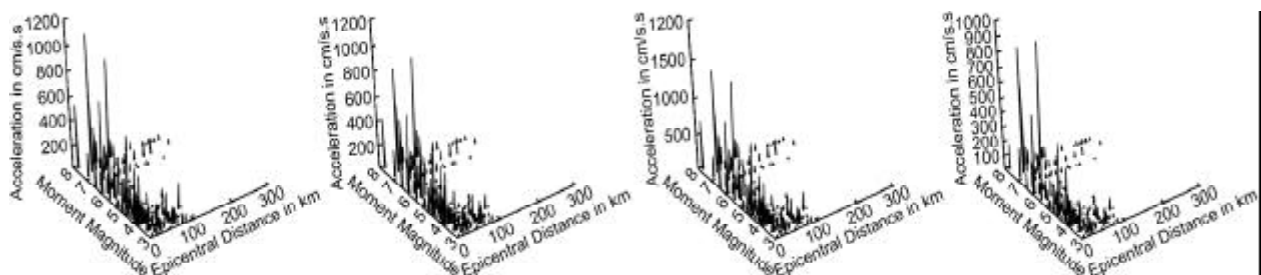

Figure 6. Three dimensional view of H1, H2, PGH and PGV acceleration.

exponential forms and non - linear logarithmic forms. Some are only presented for certain epicentral distances and magnitudes; others have focal depth as additional parameters. Also, some have terms for site conditions and source mechanisms [8-10,24,35-40]. For acceleration in Iran, Zare [20] presented exponential forms of attenuation relations. His equations have predominant ground period as an additional parameter. He also presented attenuation relations with site conditions as additional parameters [8,9].

Acceleration at the source depends on the source mechanism (type of faulting), magnitude of the earthquake and elastic properties of source media. By the time an accelerometer records the acceleration many factors may affect it. Between source and recording sites geometric spreading, refraction, reflection, scattering, diffraction, distance scaling, an-elastic absorption, site conditions, site topography, directivity, and soil amplification, affect accelerations. Thus, plot of accelerations with epicentral distances show a wide variation in ground motions for a given magnitude and distance and there is not a unique functional relation between them [32].

Recorded peak ground accelerations often have lognormal or near lognormal distribution, [23,24]; thus, assuming A as peak horizontal, or peak vertical accelerations, an equation is used in the form of

$$Ln(A) = c1 + c2*M + c3*Ln(R) + c4*R + c5*S + c6*F + E \qquad (1)$$

In Eq. (1):

$$R = r + c7*exp(c8*M), \qquad \text{or} \qquad (2)$$

$$R = sqrt(r^2 + (c7 + exp(c8*M)^2)). \qquad (3)$$

Boore, et al [40,41] and Spudich, et al [27] used another functional form given by

$$Ln(A) = c1 + c2*(M-6) + c3*Ln(R) + c4*S + c5*(M-6)2 + c6*R + c7*F + E \qquad (4)$$

Where R is defined by

$$R = sqrt(r^2 + h^2). \qquad (5)$$

Where Ln is normal logarithm; $c1$ to $c8$ are constants and are determined by regression analysis and may be positive or negative; M is the magnitude in this case $M = Mw$; F is faulting mechanism; a function expressing ground motion at the source [26]; R is a generic distance from the source, often epicentral distance plus a constant term called Joyner-Boore

distance [27]. The terms with parameter R may describe the effects during travel path from source to receiver, such as geometrical spreading, diffraction, scattering, and an elastic absorption. The terms containing $(Mw - 6)$ and $(Mw - 6)^2$ are related to saturation and distance scaling characteristics. Instead 6 values from 5 to 8.5 are also used [42]. Distance r is the epicentral distance (EPD) or distance between the accelerometer and the seismic source; parameter S indicates the site effect and E is an error term. Although in above equations 8 constants are identified, there are some other variations of these equations with up to 17 constants [24,42].

The following model is used:

$$Ln(A) = c1 + c2*(M-6) + c3 Ln(sqrt(EPD^2 + h^2)) + c4*S + c5(M-6)^2 c6*EPD + c7*F + E \qquad (6)$$

Where A may be PGH, or PGV accelerations and "$sqrt$" stands for square root function and h is the Boore-Joyner distance. However, the term F was not used, because data set was not complete.

4. Method of Analysis

SYSTAT 7.0 software was used for regression analysis and the program was checked by an artificial data set of 168 accelerations calculated based on model of Spudich et al [27] with $1 < EPD < 1000km$, $3 < Mw < 8$ and $S = 1$. Both two stages and general least square procedures were used. Results of regression procedures of both methods returned the exact coefficients of the model. Standard errors for the coefficients, p-values, standard error of regression, residual sum of squares were all zeroes, but t-ratios had very large value and the correlation coefficients were one. When EPD and $(M-6)^2$ parameters were included in the analysis, the t-ratios had small values of less than one and p-values were larger than 0.47. A p-value of 0.47 means the value of this coefficient is not differing from zero by a chance of 47%.

These results were used as a guide for regression analysis and interpretation of real data reported in this work. When t-ratios were less than one and p-values were larger than 0.47, their effect on the model was neglected.

Three analyses were performed. In the first analysis, the site effects was neglected. In the second analysis the site effects was considered by combining site group 1 and 2 together and were called firm rock sites with a numerical value of zero and combined site group 3 and 4 together and soft soil sites with a numerical value of one. This is more in line with the

recent works [24,27,42]. In the third analysis the site parameter had value of 1, 2, 3 and 4 as originally presented in the Iranian acceleration data bank. In addition, the effect of focal depth was not considered, because many were artificially kept at $33km$. After some attempts for estimating the value of h, a value $10km$ was adopted. The parameter h as an independent variable provided a wide confidence interval, from near 1 to about $40km$. The $10km$ adopted is near the major pick in depth frequency. Thus, the independent variables are Ln (PGH) and LN (PGV) and in this model dependent variables are (Mw-6), and $R = sqrt$ ($EPD^2 + 10^2$), S, (M-6)^2 and EPD. The coefficient of (M-6)^2 and EPD were small and statistically unreliable because they had small t-ratios and high p-values; thus, their values were neglected and not reported.

For the first case the results are

$$Ln\,(PGH) = 8.235 + 1.244\,(Mw\text{-}6) -$$
$$1.087*Ln\,(sqrt\,(EPD^2 + 10^2)), \text{ and} \qquad (7)$$

$$Ln\,(PGV) = 7.391 + 1.225\,(Mw\text{-}6) -$$
$$1.073*Ln\,(sqrt\,(EPD^2 + 10^2)). \qquad (8)$$

Where "$sqrt$" stands for square root, the standard error of regressions are equal to 0.855 and 0.777 and the correlation coefficients are 0.635 and 0.675 respectively.

For the second case the results are

$$Ln\,(PGH) = 8.283 + 1.255\,(Mw\text{-}6) - 1.142*Ln$$
$$(sqrt\,(EPD^2 + 10^2)) + 0.414*S, \text{ and} \qquad (9)$$

$$Ln\,(PGV) = 7.416 + 1.231\,(Mw\text{-}6) - 1.101*Ln$$
$$(sqrt\,(EPD^2 + 10^2)) + 0.214*S. \qquad (10)$$

Where parameter "S" is the site condition and can assume value 0 for firm rock, and 1 for soft soil. For this case standard error of regressions are equal to 0.836 and 0.775 and the correlation coefficient are 0.661 and 0.673 respectively.

For third case the results are

$$Ln\,(PGH) = 7.969 + 1.220\,(Mw\text{-}6) - 1.131*Ln$$
$$(sqrt\,(EPD^2 + 10^2)) + 0.212*S, \text{ and} \qquad (11)$$

$$Ln\,(PGV) = 7.262 + 1.214\,(Mw\text{-}6) - 1094*Ln$$
$$(sqrt\,(EPD^2 + 10^2)) + 0.103*S. \qquad (12)$$

Where parameter S can assume value 1 for hard rock, 2 for hard rock and thin layer of soft-top soil, 3 for gravel and sandy soil and 4 for soft soil. For this

case standard error of regressions are equal to 0.825 and 0.773 and the correlation coefficients are 0.672 and 0.675 respectively. In above equations PGH, PGV are peak ground horizontal and vertical accelerations in cm/s^2, Mw and EPD are recalculated moment magnitudes and epicentral distances in km respectively.

The statistical properties of the coefficient for each case are presented in Tables (1), (2) and (3). Tables include the coefficient value, standard error of the coefficient, t-ratios, p-values, F-test, standard error of regression, regression sum of the squares, multiple correlation coefficient, R-squared, adjusted R-squared, un-centered R-squared and the corresponding correlation coefficients. As tables indicate all three models pass the statistical F-tests. The coefficients have relatively high t-ratios and p-values are zero. However, when parameters S are included, their p-values are not zero, but vary from 0.007 to 0.211. Thus, it may be concluded that some of the site classification are not correct. Zare [20] reports that there are errors in some of the site classifications and faulting mechanisms in the Iranian data bank.

Figure (7) presents the effect of site conditions on PGH and PGV accelerations for $Mw = 6.6$ calculated based on Eqs. (7) through (12). The attenuation relations are similar in shape as expected; the soft soil, S=4, have the highest acceleration while the firm rock, S=0 have the lowest acceleration and others fall in between. Figure (8) presents PGH and PGV accelerations for $3.5 = < Mw = < 7.5$ for site conditions $S = 0$ and $S = 4$. The upper panel shows the PGH accelerations and the lower panel shows the PGV acceleration respectively.

5. Comparison of Observations and Predictions

To compare the observations and predictions or calculations, a series of plots are needed. Figure (9) presents plots of actual 279 observed PGH and PGV accelerations in the upper and lower panels respectively. The left pairs are based on Eqs. (7) and (8) where no site conditions were used. The middle pairs are based on equations 9 and 10 when S = 0 or 1 for firm rock and for soft soil respectively. The right pairs are based on equations 11 and 12 where site parameter S varies from 1 to 4 depending on site conditions. The dots are the position of the calculated accelerations for the reported epicentral distances and magnitudes. Dashed lines and solid lines are contour values of moment magnitudes, Mw.

Plots for several magnitude rangs were also produced in some areas and were combined in order to

Table 1. Model and statistical properties of constant and coefficients: case A for PGH and Case B for PGV: Site conditions are not considered.

Model: $Ln(ACC) = c1 + c2*(Mw-6) + c3*Ln(sqrt(EPD^2+10^2)))$

Case A

ACC: PGH acceleration

	Parameter	Estimate	S.E.	t-Ratio	P-Value
1	c1	8.235	0.514	16.016	0.000
2	c2	1.244	0.209	5.957	0.000
3	c3	-1.087	0.142	-0.7.66	0.000

F (3,274) = 29.774481, prob. = 0.00000

Standard error of regression: 0.855087

Regression sum of squares: 43.540609

Residual sum of squares: 64.343248

R-squared: 0.403588, Adjusted R-squared: 0.390033, Un-centered R-squared: 0.966433.

The correlation coefficients are 0.635, 0.624 and 0.983 respectively.

Model: $Ln(ACC) = c1 + c2*(Mw-6) + c3*Ln(sqrt(EPD^2+10^2)))$

Case B

ACC: PGV acceleration

	Parameter	Estimate	S.E.	t-Ratio	P-Value
1	c1	7.391	0.467	15.811	0.000
2	c1	1.225	0.190	6.457	0.000
3	c2	-1.073	0.129	-0.8.314	0.000

F (3,274) = 35.061892, prob. = 0.00000

Standard error of regression: 0.777401

Regression sum of squares: 42.379521

Residual sum of squares: 53.183056

R-squared: 0.45611, Adjusted R-squared: 0.437355, Un-centered R-squared: 0.96054.

The correlation coefficients are 0.675, 0.661 and 0.998 respectively.

Table 2. Model and statistical properties of constant and coefficients: case A for PGH and Case B for PGV: Site conditions are considered; S is 0 for hard rock and 1 for soft soil.

Model: $Ln(ACC) = c1 + c2*(Mw-6) + c3*Ln(sqrt(EPD^2+10^2))) + c4*S$

Case A

ACC: PGH acceleration

	Parameter	Estimate	S.E.	t-Ratio	P-Value
1	c1	8.283	0.503	16.465	0.000
2	c2	1.255	0.204	6.148	0.000
3	c3	-1.42	0.141	-.8.106	0.000
4	c4	0.414	0.183	2.254	0.027

F (3,274) = 17.385958, prob. = 0.00000

Standard error of regression: 0.783822

Regression sum of squares: 42.726146

Residual sum of squares: 52.83.6440

R-squared: 0.436508, Adjusted R-squared: 0.417077, Un-centered R-squared: 0.968286.

The correlation coefficients are 0.661, 0.646 and 0.984 respectively.

Model: $Ln(ACC) = c1 + c2*(Mw-6) + c3*Ln(sqrt(EPD^2+10^2))) + c4*S$

Case B

ACC: PGV acceleration

	Parameter	Estimate	S.E.	t-Ratio	P-Value
1	c1	7.416	0.466	15.903	0.000
2	c2	1.231	0.189	6.507	0.000
3	c3	-1.101	0.131	-8.434	0.000
4	c4	0.214	0.170	1.259	0.211

F (3,274) = 22.464756, prob. = 0.00000

Standard error of regression: 0.835916

Regression sum of squares: 47.092121

Residual sum of squares: 60.791736

R-squared: 0.453436, Adjusted R-squared: 0.434589, Un-centered R-squared: 0.960346.

The correlation coefficients are 0.673, 0.659 and 0.980 respectively.

Table 3. Model and statistical properties of constant and coefficients: case A for PGH and Case B for PGV: Site conditions are considered; S is 1 for hard rock and 2 hard alluvial and soft thin top soil, 3 for gravel and sandy soil and 4 for soft soil.

Model: $Ln(ACC) = c1 + c2*(Mw-6) + c3*Ln(sqrt(EPD^2+10^2))) + c4*S$

Case A

ACC: PGH acceleration

	Parameter	Estimate	S.E.	t-Ratio	P-Value
1	c1	7.969	0.505	15.778	0.000
2	c2	1.220	0.202	6.053	0.000
3	c3	-1.31	0.138	-.8.206	0.000
4	c4	0.212	0.077	2.761	0.007

F (3,274) = 23.884226, prob. = 0.00000

Standard error of regression: 0.824621   Regression sum of squares: 48.723838   Residual sum of squares: 59.160020

Model: $Ln(ACC) = c1 + c2*(Mw-6) + c3*Ln(sqrt(EPD^2+10^2))) + c4*S$

R-squared: 0.451632, Adjusted R-squared: 0.432723, Un-centered R-squared: 0.969137.

The correlation coefficients are 0.672, 0.658 and 0.984 respectively.

Case B

ACC: PGV acceleration

	Parameter	Estimate	S.E.	t-Ratio	P-Value
1	c1	7.262	0.473	15.340	0.000
2	c2	1.214	0.189	6.427	0.000
3	c3	-1.094	0.129	-8.469	0.000
4	c4	0.103	0.072	1.422	0.159

F (3,274) = 24.319584, prob. = 0.00000

Standard error of regression: 0.772930   Regression sum of squares: 43.587030   Residual sum of squares: 51.975556

R-squared: 0.456110, Adjusted R-squared: 0.437355, Un-centered R-squared: 0.96054.

The correlation coefficients are 0.675, 0.661 and 0.980 respectively.

Note in all analyses the coefficients c5, c6 had small t-ratios and high p-value; thus, they are neglected.
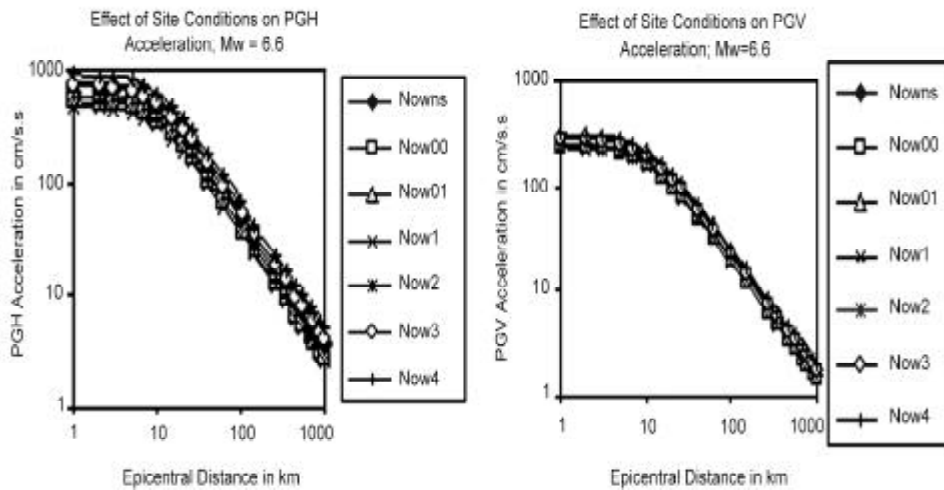
Figure 7. Ground attenuation for PGH and PGV acceleration from this study for Mw=6.6. Effects of site conditions are shown by ns, 00, 01, 1, 2, 3 and 4 affixed to NOW. The affixes mean calculations are for cases with, no site conditions, firm rock site, soft soil site, rock site, thin soft alluvial sites, sandy gravel sites and deep soft soil sites. As Mw=6.6 is adopted for the Bam earthquake of 2003, this figure may present a prediction for acceleration attenuation for this event. The rock site, 00, has the lowest and deep soil site, 4, has the highest predicted acceleration. Other site conditions are in between.
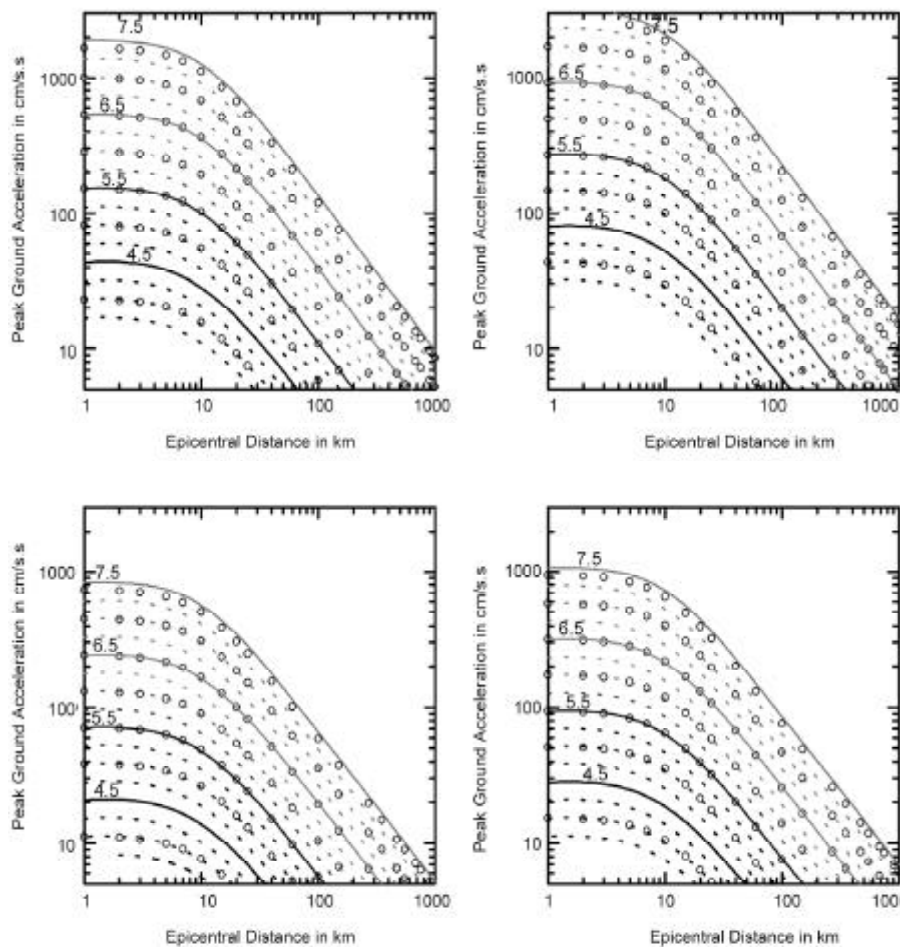

Figure 8. Predicted PGH, upper panel, and PGV lower panel for 3.5=<Mw=<7.5 and site conditions, S=0, and S = 4. The small circle shows the position of a data point for a given magnitude; epicentral distance and Mw, the dashed lines and solid lines are contours of moment magnitude Mw.
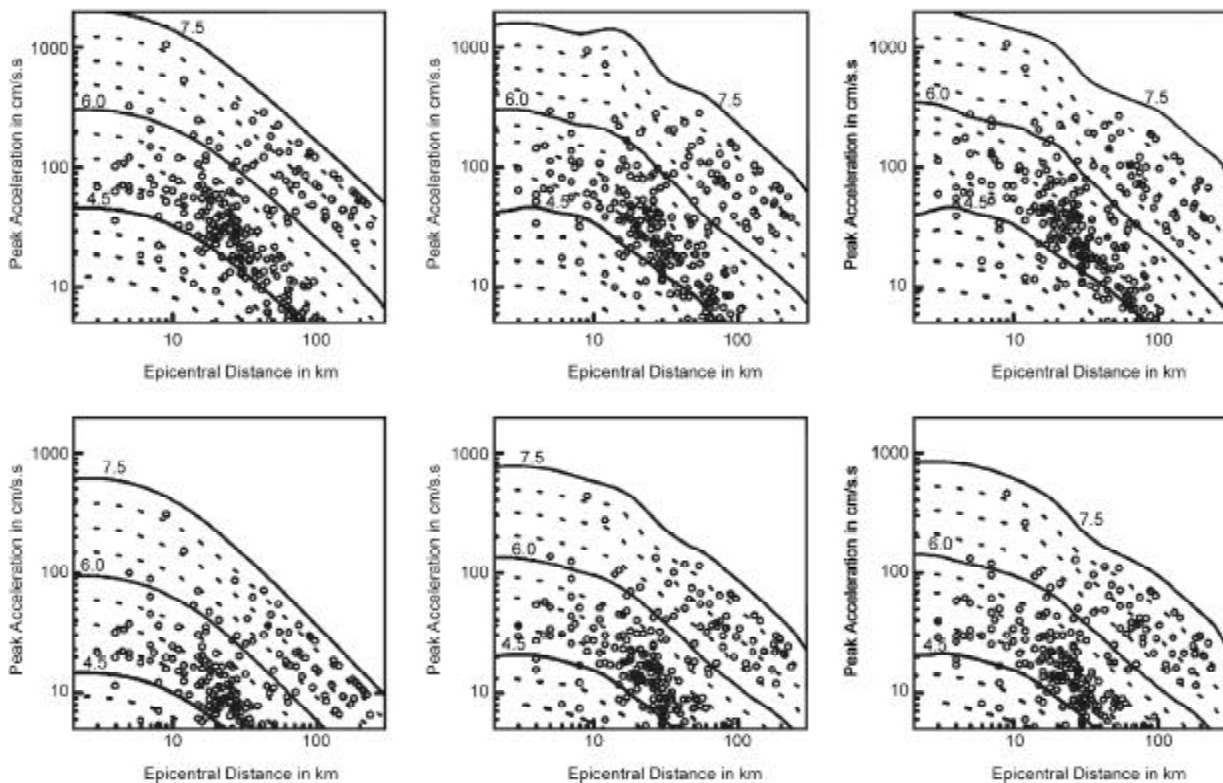
Figure 9. This figure represents a plot of calculated PGH and PGV acceleration in the upper and lower panel respectively. Calculations are based on equation 7 -12 respectively. Site conditions are not used in the first left pairs; S = 0, or 1 for middle pairs and; S = 1- 4 are used for the right pairs. Again the small circles show the position of calculated data points; dashed line and solid lines show the contour values of Mw.

have sufficient data for plotting. To be brief in Figure (10), only the plots of observed and calculated *PGH* and *PGV* accelerations were presented for *Mw* = 6.1 to 6.5. Other magnitude ranges provide similar plots and are not presented. The calculations include plus and minus one standard deviation. The agreements are relatively good. The figures indicate that only a few points fall outside of the predicted range. The reasons may be due to the complexity of travel paths, site conditions, focal mechanisms, and directivity effects. These factors were not used in this work.

6. Ratio of Vertical to Horizontal Acceleration

In practical engineering design, the value of peak ground vertical acceleration is often assumed to be the 2/3 of the peak ground horizontal acceleration. The observed ratios for Iranian earthquakes are rather different. The ranges of ratios vary from a small value of 0.02 to 2.52. However, the average ratio for all 279 records is about 0.5. There are six records showing ratios higher than one. The station names, epicentral distances, and surface wave magnitudes, *Ms* are as follows: Kazerun, 45*km*, 5.6; Sharif University, 210 *km*, 7.7; Shabastar, 16*km*, 3.5; Gachsar, 185*km*, 7.7; Dez Dam, 8*km*, 5.1; and Abbar 63*km*,
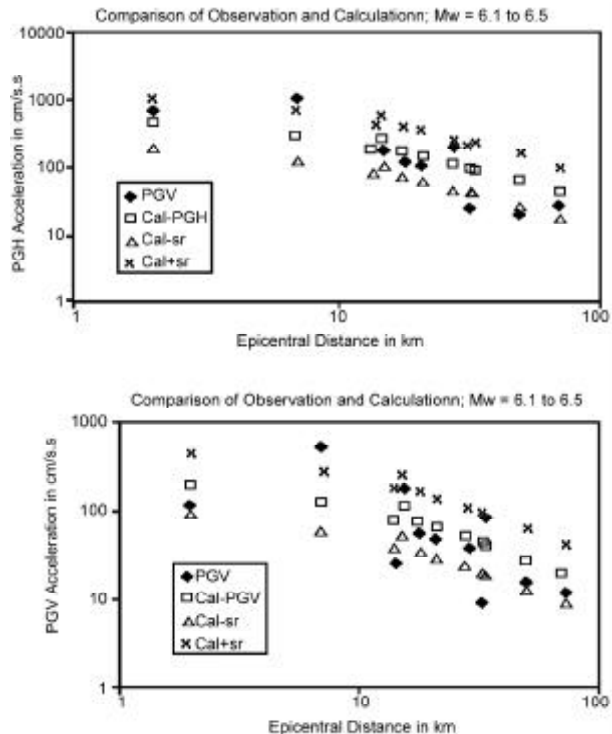

Figure 10. Comparison between observed PGH, and PGV accelerations and calculated value based on equation 7 and 8 for 6.1 =< MW =< 6.5. Diamond, square, triangle and cross symbols represent observed and calculated accelerations; and plus and minus one standard error of regression respectively.

4.1 respectively. It is interesting to note that no clear correlation exists between increase of ratio and magnitude or epicentral distances. However, many large magnitude events have a ratio of about 0.6 to 0.7. A pictorial plot of observed ratios as a function of moment magnitude and epicentral distance is presented in Figure (11). While Figure (12) shows the frequency distribution of observed ratio, a majority of ratios are between 0.3 to 0.7 and there are a few outliers outside the plotted range and are not shown.

7. Comparison with Other Studies

A large number of attenuation relations are reported in the literature [35,23,31,20,8,9,24,42,40]. An attempt was made to compare the results of this work with some of the recent literature. An exact correspondence and equality among the results with other authors, or equality of the results of other authors among

Figure 11. This figure shows the observed PGV/PGH ratio as a function of Mw and Epicentral distances.

Figure 12. This figure shows the observed frequency distribution of PGV/PGH ration.

themselves was not expected; because, little agreements have been achieved in the last three decades of ground motion estimation relation studies [32]. The purposes are limited only to find the range of variations between the obtained results and others findings. For comparison, the attenuation equations proposed by several authors were used. They are: Boore et al [37] for Western United States, but dominated by data from California; [16] for the Manjil earthquake in Iran, *Ms*=7.7; Fukushima et al [43] for Japan; Campbell and Bozorgnia [24] and Spudich et al [27] for worldwide application; Zare [8], and Zare [20] for Iran. Niazi and Bozorgnia [16] proposed three models in the form of Ln (*PGH*) = *a* +*d**Ln (*EPD* + *c*) for the Manjil earthquake with *Ms* = 7.7. They presented values for constants *a*, *d*, *c*, and standard deviation for each model. Their model 2 with constants *a* =2.03, *d* =-1.05 and *c* =5.82 has the lowest standard deviation. Thus, this model is adopted for comparison. This model was developed only as *Ms* = 7.7, and it is not valid for any other magnitude, because magnitude is not a parameter in the model. The model proposed by Campbell and Bozorgnia [24] is the most complete with 17 coefficients which has adjustment terms for faulting mechanisms, local site conditions, effect of the hanging wall of the source faulting; in addition to scaling magnitude and distant characteristics. A firm ground and thrust faulting in calculation using this model was assumed. Zare [20] presented three attenuation equations for Central Iran Alborz/Lut, Eastern Iran, and the Zagros regions. He has used predominant period as additional parameters. This parameter is constant up to 40*km*. A predominant period of 0.22 second using his graph was used. My calculations for his models are carried out up to this distance. Zare [8] and Zare et al [9] and Spudich et al [27] considered site condition as additional parameter. In this comparison, a hard rock for using their equations is assumed. The attenuation equations proposed by all authors may be used for any magnitude range of 5 to 7.7. Thus, a direct comparison assuming *Mw* = 7.0 and, *Mw* = 5.0 was made. For *Mw* = 7.0, and firm site condition, Figure (13) shows that, for *Mw* = 7.0, the *PGH* and *PGV* accelerations attenuation with distance have nearly similar shape. But, the results of this work show higher *PGH* acceleration, because vectorial summation of horizontal components for calculations of PGH acceleration was used. In the other works, often, the mean of two horizontal components are used. However as Zare [8] and Zare et al [9] formulations do not include
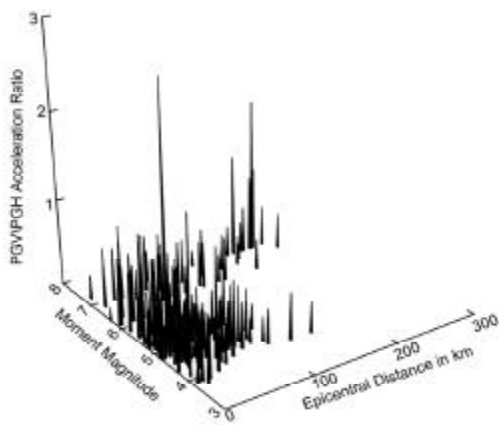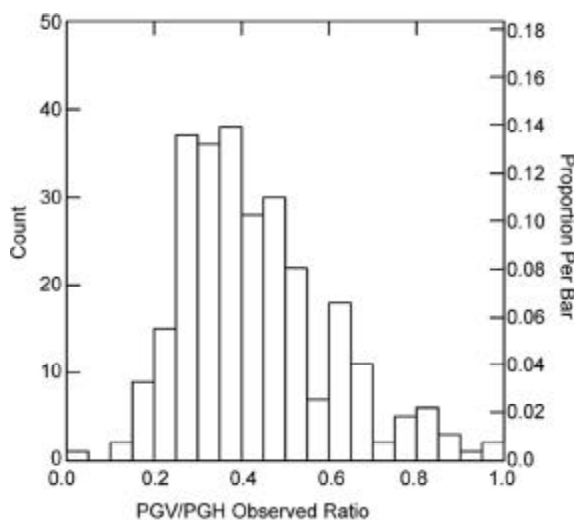
a saturation term and their equations yield even higher acceleration at near source region. But, at this region, the results of Zare [20] are slightly lower than results of Campbell and Bozorgnia (2003) and are more like results of Boore and Joyner [41]. Also Equation of Fukushima et al [43] and Boore and Joyner [41] yield lower acceleration at epicentral distances of more than about 100*km* (Figure (13), upper panel).

For $Mw = 7.0$, a comparison of the results of *PGV* acceleration between this work and those of Zare [8], and Campbell and Bozorgnia [24] is also presented, (Figure (13), lower panel). The *PGV* accelerations of this work are in relatively good agreement with Campbell and Bozorgnia, but at near source distances. Zare (1999) results show higher values; because, he has not included the saturation term.

The *PGH* and *PGV* accelerations for $Mw = 5.0$ shows more contrast. In the near source region, $(1 < EPD < 10 km)$, the estimated *PGH* acceleration in this work is lower than the results of other investigators; however, for larger distances they are about the same. Over all, the obtained results are similar to

results of Spudich et al [27]. For epicentral distance of less than $5 km$, results of Boore and Joyner [41] and results of Zare [20] are similar; and results of Fukushima et al [43] and Campbell and Bozorgnia [24] are about the same (Figure (14), upper panel). The *PGV* acceleration predicted for $Mw = 5.0$ is about the same for distances larger than about 20 Km but for smaller distances. Zare [8] and Campbell and Bozorgnia [24] predicted higher accelerations (Figure (14), lower panel).

A summary of differences may be expressed in terms of numbers. As an example, for $Mw = 7.0$, $EPD = 5 km$, and firm rock, the *PGH* acceleration in this paper is 792.19*cm/s.s*, while for models of Zare et al [9], Campbell and Bozorgnia [24], Fukushima et al [43], and Spudich et al [27]. They are 800.81, 787.94, 519.74, 393.42 cm/s.s respectively; at $EPD = 270 km$. The results of this paper is 21.55*cm/s.s*, while other models predict 12.35, 18.72, 6.36, 10.75*cm/s.s* respectively. For $Mw = 5.0$, $EPD = 5 km$, the PGH accelerations are 108.64, 153.65, 314.51, 246.87, 99.29*cm/s.s* for this paper and other authors respectively and

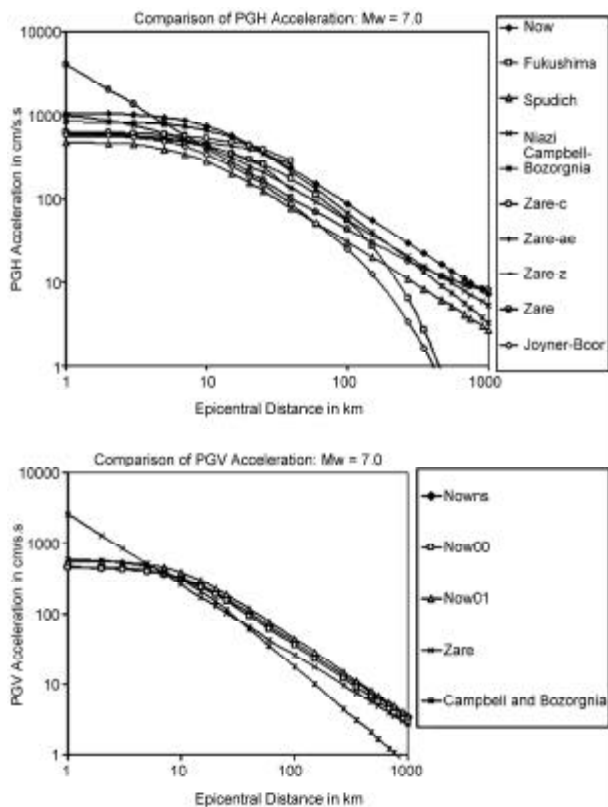**Figure 13.** Comparison between calculations of PGH and PGV accelerations for several models for Mw =7.0. Abbreviations are: Now, Nowns, Now00 and Now01 from this work, Fukushima et al [43], Spudich et al [27], Niazi and Bozorgnia [16], Zare [20], Zare [8] Boore and Joyner [40], Campbell and Bozorgnia [24].
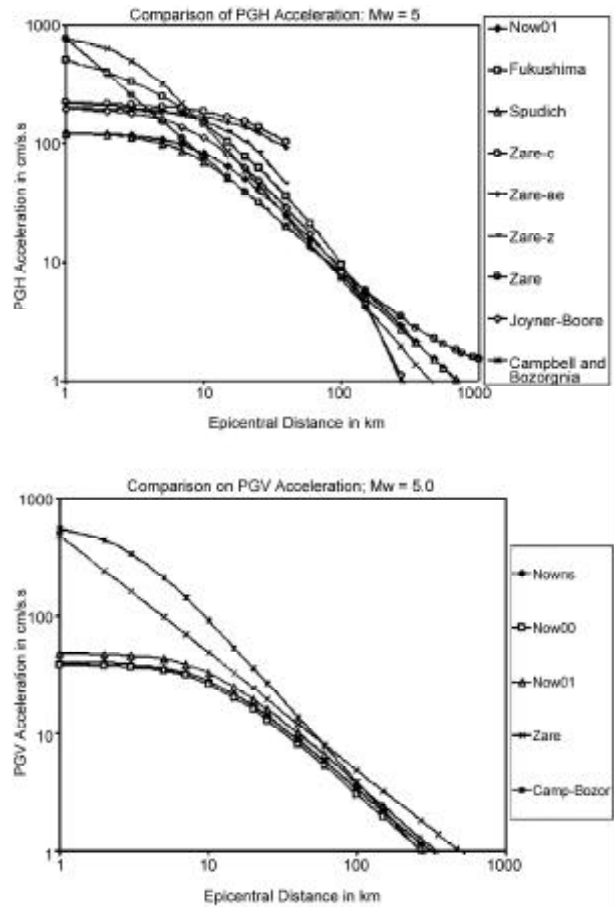
Figure 14. Comparison between calculations of PGH and PGV accelerations for several models for Mw=5.0.

finally at *EDP* = 270, the results are 2.85, 3.14, 1.93, 0.98 and 2.71*cm/s.s* respectively. Thus, the variations in *PGH* acceleration estimations not only depend on magnitude and epicentral distances but also on the models as well.

8. Assessment of the Bam Earthquake Magnitude, Seismic Moment and Near Source Accelerations

According to the United State Geological Survey, National Earthquake Information Center [44], a strong earthquake occurred at 01:56:52.44 (*UT*), on 26 December 2003 with the latitude, longitude and depth of: 29.004 North, 58.337 West and 10*km* respectively. The earthquake magnitudes were: *Ms* = 6.8 and *Mw* = 6.6. The best double couple moment is 8.6*10²⁵*dyne-cm* corresponding to *Mw* = 6.5.

The source is the strike slip Bam fault with a length of about 110*km* tending about 15 degree west of north (Tectonic map of southeast Iran, National Iranian Oil company, 1977). The Bam earthquake was not unexpected. Nowroozi and Mohajer [45] considered the Bam fault as a seismogenic fault. In addition, Nowroozi [1] used the concept of seismotectonic province where each province has a uniform risk. The city of Bam and Bam fault are in the Lut province as defined by Nowroozi [3]. In this province, the return period of an earthquake with magnitude 7 was reported as 269 years. In addition at 20*km* focal distance for 200 years time exposure, the expected acceleration was 0.22*g* [1]. Thus, clearly city of Bam was at risk, although, the seismic risk was underestimated.

An approximate magnitude and seismic moment of this earthquake could have been estimated prior to the event. Nowroozi [46] developed empirical relations between fault length, *L*, seismic moment, *Mo*, and the and surface wave magnitude *Ms*. These equations are

$$Ms = 1.259 + 1.244 * \log L, \tag{13}$$

and

$$Mo = 14.354 + 1.733 * Ms \tag{14}$$

Where *L* is in meters and *Mo* is in dyne-cm. As fault length is 110,000 meters, equation 13 yields an estimate of *Ms* equal to 7.5. This Magnitude is predicted if the entire fault length of 110*km* was activated, thus, it is the maximum capability of this fault. It is believed that any critical structure in the city of Bam that is near the Bam fault ought to be designed for this potential magnitude. However, often only a portion of a strike-slip fault is activated; assuming

30% of the fault length or 33*km* was activated, Eq. (13) predict *Ms* = 6.9. This is in agreement with the reported *Ms* magnitude of 6.8 for this event. Tatar et al [47] reported the aftershock distribution is consistent with a 30*km* length along the Bam fault. Assuming a fault length of 30*km* Eq. (13) predicts a surface magnitude of 6.82 or nearly the same as reported magnitude. Harvard Seismology Center [48] also reported *Mw* = 6.6, *Ms* = 6.8, *mb* = 6.0 and seismic moment of 9.31*10²⁵ *dyne-cm*. Mostafazadeh et al [49] estimated a total seismic moment of 8.34*10¹⁸ *Nm* or 8.34*10²⁵ *dyne-cm* for the main event and smaller value for the second event. USGS [44] also gave 10*10¹⁸*Nm* or 10*10²⁵*dyne-cm* for moment tensor scale of this event.

For *Ms* = 6.8, Equation 14 predict a seismic moment of 13.75*10²⁵ *dyne-cm*. This is in relatively good agreements with moment reported by USGS [44] and Harvard Seismology Center [48] and Mostafazadeh et al [49]. Using the relation *Mw* = 0.69**Ms* + 1.92, and assuming *Ms* = 6.8, it follows again that *Mw* = 6.6 is in agreement with both Harvard and USGS estimations. However, this magnitude differs slightly from *Mw* = 6.5 adopted for this event, Zare [50].

The Bam fault passes through the city; the uncorrected accelerations recorded in the city of Bam are 0.8*g* and 0.7*g* for the horizontal components and 0.98*g* for the vertical component [50], where *g* is the gravitational acceleration, or 981*cm/s.s*. Thus, using vectorial method, and converting units, the *PGH* and *PGV* accelerations are 1042.81*cm/s.s* and 961.38*cm/s.s* respectively. In Figure (7), based on Eqs. (7-12), the expected *PGH* and *PGV* acceleration attenuation plots for an earthquake is shown with moment magnitude *Mw* = 6.6, or for the Bam earthquake. For *S* = 4 and *EPD* < 5*km*, the predicted accelerations are 918.64 < *PGH* < 1042.28 and 318.92 < *PGV* < 360.35*cm/s.s* respectively. Thus, Eq. (11) almost predicts the *PGH* acceleration for the Bam recordings. However, Eq. (12) underestimates the *PGV* acceleration by a factor of about 3. The observed *PGV/PHV* ratio is 0.92. About 2% of Iranian earthquakes have similar ratios, see Figure (12). The higher than expected *PGV* accelerations, although not understood, may be due to soil amplification at the recording site and the effect of vertical directivity.

9. Discussion

As Figures (13) and (14) indicate, the acceleration

estimations based on various models are not the same. In fact, Douglas [32] concluded that there has been little agreement in the past 30 years in ground motion estimation studies. Using magnitudes and epicentral distances in the Iranian acceleration data bank as parameters, see Figure (15), the estimated *PGH* and *PGV* acceleration based on several models has been plotted. On the x- axes, the estimations are based on Eqs. (11) and (12) for *PGH* and *PGV* accelerations respectively is plotted. On the y-axis the estimations are based on relations proposed by other authors. If estimations were nearly the same all points would have been on the diagonal lines. However, the data points are scattered about the lines that are plots of Eqs. (11) and (12) against itself or the author's estimations. Thus, there are differences between these estimations and results of the other authors. In addition, there are variations among results of other authors for both *PGH* and *PGV* accelerations. For any acceleration on the x- axes, a range of acceleration can be read on the y- axes. This range is a measure of variations among estimations. As an example for $Mw = 7.0$ and at $EDP = 5km$ this range for *PGH* accelerations is between 393.42 to 1338.86 $cm/s.s$ depending on models and site conditions. For the same magnitude and distance, the range for *PGV* acceleration is between 400.53 to 514.20 $cm/s.s$. Better models, data and more parameters are required to reduce this range of variations.

Eqs. (7) to (12) ought to be used with care. Eqs. (7) and (8) are more useful for cases that site conditions are not known. Eqs. (9) and (10) are useful when site conditions are firm rock or soft soil and, finally Eqs. (11) and (12) are useful if the condition of the site is fully known, as reported in Iranian acceleration data bank. However, when site conditions are used as additional parameters the coefficient for *S* has high p-values and smaller t-ratios which indicates that site classification may be in error in some cases. Zare [20] questioned the validity of site conditions and source mechanisms of many of the published data. Thus, there is more confidence in results of Eqs. (7) and (8) than others.

The epicentral distances varied between 2 to 245 km; thus, equations 7-12 are basically valid for this range. Although, the equations may provide some reasonable acceleration even at near source zone *EPD* <5km, no structure is recommended to be constructed at these distances based on the acceleration obtained from these equations. Common sense demands that no critical structures, such as power plants, hospitals,
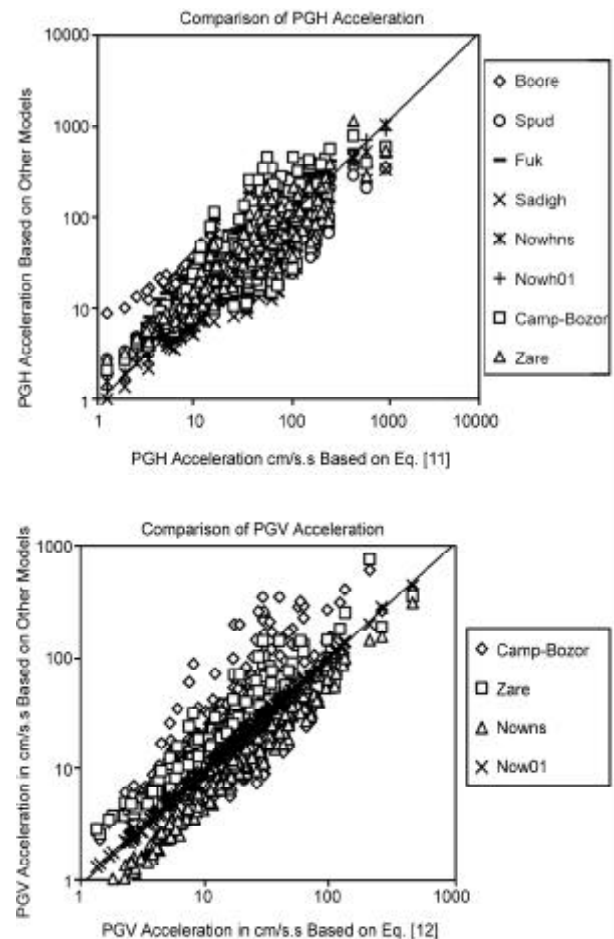
Figure 15. Comparison between 279 observed PGH and PGV accelerations calculated based on Eqs. (11) and 12 respectively and results of several models. Abbreviations for Models are: Boore and Joyner [40]; Spudich et al [27]; Sadigh et al [38]; NOWhns, NOWh01, NOWns and NOW01, this work; Camp-Bozor, Campbell and Bozorgnia [21]; Zare, [8].

schools, airports, bridges, military facilities, industrial facilities, apartment buildings or houses be build so close to a fault. The areas that are close to a fault are better used as agricultural land or parks. But, if there are no other choices, then these equations may be used for a preliminary site assessments. A site specific study must be carried out to find the design base accelerations and dynamic analysis ought to be applied for structural designs.

10. Conclusions

Preliminary attenuation equations for *PGH* and *PGV* accelerations are developed for Iran. For $Mw = 7.0$, the shape of *PGH* acceleration attenuations in Iran is similar to shapes obtained by Campbell and Bozorgnia [24], Fukushima et al [43], Spudich et al [27], Zare [20] and Boore et al [37]. The obtained estimations in this paper are also about the same as those calculated based on some of the models.

However, the results of Zare [8] and Zare et al [9] exceed my estimations at near source region, because their formulation do not include a saturation term. In addition for distances larger than $100km$, the results of Fukushima et al [43] and Boore et al [37] is lower, but at $EPD>100km$, the accelerations are not very large. The PGV acceleration attenuation of Zare et al [9] again exceed my results for near source region.

For $Mw = 5.0$, at near source distances of up to $14km$, my estimated PGH accelerations are smaller than Fukushima et al [43], Zare [20], Campbell and Bozorgnia [24] and Zare et al [9], but it is similar to results of Spudich et al [27]. The *PGV* acceleration are nearly the same for $EPD>15km$, and smaller at near source in comparison with the results of Campbell and Bozorgnia and Zare [8].

Thus, estimations of *PGH* and *PGV* accelerations not only depend on magnitude, epicentral distances and site conditions but also depend on the proposed models.

Results of 279 *PGH* and *PGV* acceleration estimations for $3.0<Mw<7.2$ and $2<EPD<245km$ from various authors show about one order of magnitude variations, the *PGH* acceleration estimations obtained in this paper are comparable to others and there is a need for more good quality data, better models and more parameters to reduce the scatter.

Based on this work, the author was able to estimate the *PGH* and *PGV* accelerations at near source of the Bam earthquake of 26 December 2003. In the Bam city, the uncorrected recorded horizontal component of acceleration are 784.8 and 686.7$cm/s.s$ respectively; thus, the *PGH* acceleration is 1042.82$cm/s.s$ and recorded *PGV* acceleration is 961.38$cm/s.s.$ The obtained estimations in this paper are $918.64 < PGH <1042.28$ and $318.92 < PGV <360.35cm/s.s$ respectively. Thus, the recorded PGH acceleration is in agreement with the estimation, but the *PGV* acceleration is lower by a factor of about 3. The *PGV/PGH* ratio of this event is 0.92. About 2% of Iranian earthquakes have a *PGV/PGH* ratio of about 0.9 and the high ratios may be due to soil amplification and source directivity that are not parameterized in this work.

Acknowledgements

References

1. Nowroozi, A.A. (1987). "Tectonics and Earthquake Risk in Iran", In: Ground Motion and Engineering Seismology, (ed. Cakmak, A. A), Elsevier, 59-75.

2. Nowroozi, A.A. and Ahmadi, G. (1986). "Analysis of Earthquake Risk in Iran Based on Seismotectonic Provinces", *Tectonophysics,* **122**, 89-114, Elsevier.

3. Nowroozi, A.A. (1976). "Seismotectonics Provinces of Iran", *Bulletin of the Seismological Society of America*, **66**, 1249-1276.

4. United States Geological Survey Website (2004). http://earthquake.usgs.gov/.

5. Decannini L., and Mollaiolli F., (1999). "Formulation of the Elastic Input Energy Spectra", *Earthquake Engineering and Structural Dynamics*, 27, 1503-1522.

6. Building and Housing Research Center (1993). "A Collection of the Accelerograms Network of the Islamic Republic of Iran, **179**, 173 p.

7. Bard, P., Zare, M., and Ghafory-Ashtiany, M. (1998). "The Iranian Acceleration Data Bank: A Revision and Data Correction", *Journal of Seismology and Earthquake Engineering*, **1**, 1-21.

8. Zare, M. (1999). 'Contribution a' l' E'tude des Mouvements Forts en Iran; du Catalogue Aux Lois D'atte'nuation", Observatoire de Grenoble et Laboratoire de Geogphysique Interne et Tectoniphysique, L' Universite' Joseph Fourier - Grenoble I.

9. Zare, M., Ghafory-Ashtiany, M., and Bard, P. (1999). "Attenuation Law for the Strong Motions in Iran", *Proceedings of the Third International Conference on Seismology and Earthquake Engineering*, Tehran, Iran, 345-354.

10. Trifunac, M.D. (1976). "Preliminary Analysis of the Peaks of Strong Earthquake Ground Motion-Dependence of Peaks on Earthquake Magnitude, Epicentral Distance and Recording Site Conditions", *Bulletin of the Seismological Society of America*, **66**(1), 189-219.

11. Lay, T. and Wallace, T. (1995). "Modern Global Seismology", Academic Press, New York.

12. Moinfar, A.A. and Adibnazari, H. (1982). "The Tabas Earthquake of September 16, 1978", Building and Housing Research Center, Islamic Republic of Iran, Technical Report No. 47.

13. Moinfar, A.A. and Eetemadi, M. (1982). "Acceleration of Golbaft-Sirch 1982 Earthquake", Building and Housing Research Center, Islamic Republic of Iran, Internal Report.

14. Shoja-Taheri, J. (1984). "Acceleration of the 1978 Tabas (Iran) Earthquake: The Generalized Records of Correlation between the Strong Motion Parameters in Different Frequency Bands", An Oral Presentation at Regional Assembly of IASPEI, Heyderabad, India.

15. Niazi, M. (1986). "Acceleration of 1978 Tabas, Iran Earthquake", *Earthquake Spectra*, **2**, 635-651.

16. Niazi, M. and Bozorgnia, Y. (1992). "The 1990 Manjil, Iran Earthquake: Geology and Seismology Overview, PGA Attenuation, and Observed Damage", *Bulletin of the Seismological Society of America*, **82**(2), 774-799.

17. Shoja-Taheri, J. and Anderson, J. (1988). "The 1978 Tabas, Iran, Earthquake: An Interpretation of the Strong Motion Records", *Bulletin of the Seismological Society of America*, **78**, 142-171.

18. Moinfar, A. A. and Naderzadeh, A. (1990). "An Immediate and Preliminary Report on the Manjil Iran Earthquake of 2 June 1990", Building and Housing Research Center, Islamic Republic of Iran, Report No.119, 68 p.

19. Saikia, C.K. (1994). "Modeling of Strong Ground Motions from the 16 September 1978 Tabas, Iran Earthquake", *Bulletin of the Seismological Society of America*, **84**, 31-46.

20. Zare, M. (1995). "Site Dependent Attenuation of Strong Motions for Iran", *Proceedings of the Fifth International Conference on Seismic Zonation*, Nice, France, 1227-1236.

21. Campbell, K.W. and Bozorgnia, Y. (1994). "Near Source Attenuation of Peak Horizontal Acceleration from Worldwide Accelerograms Recorded from 1957 to 1993", *Fifth US. National Conference on Earthquake Engineering*, Chicago.

22. Maggi, A., Priestley, K. and Jackson, J. (2002). "Focal Depths of Moderate to Large Earthquakes in Iran", *Journal of Seismology and Earthquake Engineering*, **4**(2-3), 1-10.

23. Campbell, K.W. (1985). "Strong Motion Attenuation Relations: A Ten-Year Perspective", *Earthquake Spectra*, **4**, 759-804.

24. Campbell, K.W. and Bozorgnia, Y. (2003). "Updated Near-Source Ground-Motion (Attenuation) Relations for the Horizontal and Vertical Components of Peal Ground Acceleration and Acceleration Response Spectra", *Bulletin of the Seismological Society of America*, **93**(1), 314-331.

25. Panza, G.F., Romanelli, F., Vaccari, F., Decannini, L., and Mollaiolli, F., (2003), "Seismic Ground Motion Modelling and Damage Earthquake Scenarios, A Bridge between Seismologists and Seismic Engineers, OECD Workshop on the relations between Seismological Data and Seismic Engineering, Istanbul, 16-18 october 2002, Proceedings, Organisation for Economic Cooperation and Development, pp. 241-266.

26. Richter, C. (1958). "Elementary Seismology", Freeman and Company, Inc.

27. Spudich, P., Joyner, W.B., Lindh, A.G., Boore, D.M., Margaris, B.M. and Fletcher, J.B. (1999). SEA99: A Revised Ground Motion Prediction Relation for Use in Extensional Tectonic Regimes, *Bulletin of the Seismological Society of America*, **89**(5), 1156-1170.

28. Wang, H., and Nisimura, A. (1999), "On the Behavior of Near Source Strong Motion from the Seismic Records in Down-hole Array at Hyogocene-Nanbu Earthquake", Earthquake

Resistant Engineering Structures II, (G. Oliveto and C.A. Brebbia eds.), WIT Press, Boston, 363-372.

29. Romanelli, F., and Vaccari, F. (1999), "Site Response Estimation and Ground Motion Spectra Scenario in the Catania area", *Journal of Seismology*, 3, 311-326.

30. Panza, G.F., Romanelli, F., and Vaccari, F., (2001), "Seismic Wave Propagation in Laterally Heterogeneous Anelastic Media: Theory and Applications to the Seismic Zonation", Advances in Geophysics, Academic Press, 43, 195 p.

31. Leonov, J. (2003). "Horizontal Peak Ground Acceleration Attenuation Relation: Way and Argumentations of Its Choice", http://www.gii.co.il/heb/Teken/Leonov/Leom_doc.htm, 1-5.

32. Douglas, J. (2003). "Earthquake Ground Motion Estimation Using Strong-Motion Records: A Review of Equations for the Estimation of Peak Ground Acceleration and Response Spectral Ordinates", *Earth Science Review,* 6, 43-104.

33. Douglas, J. (2001). "A Critical Reappraisal of Some Problems in Engineering Seismology", PhD Thesis, University of London.

34. Douglas, J. (2002). "A Comprehensive Worldwide Summary of Strong-Motion Attenuation Relationships for Peak Ground Acceleration and Spectral Ordinates (1969 to 2000)", SM Reports, Dept. of Civil and Environmental Engineering, Imperial College London.

35. Joyner, W.B. and Boore, D.M. (1981). "Peak Horizontal Acceleration and Velocity from Strong-Motion Records Including Records from the 1979 Imperial Valley, California, Earthquake", *Bulletin of the Seismological Society of America,* 71, 2011-2038.

36. Joyner, W.B. and Boore, D.M. (1982). "Prediction of Earthquake Response Spectra", U.S. Geological Survey, Open-file Report, 82-977.

37. Boore, D.M., Joyner, W.B. and Fumal, T.E. (1997). "Equations for Estimating Horizontal Response Spectra and Peak Acceleration from Western North American Earthquakes: A Summary of Recent Work", Seismological Research Letters, **68**, 128-153.

38. Sadigh, K., Chang, C.Y., Egan, J.A. Makdisi, F., and Youngs, R.R. (1997). "Attenuation Relationship for Shallow Crustal Earthquakes Based on California Strong Motion Data", Seismological Research Letter, **68**(1), 180 p.

39. Campbell, K.W. (1997). "Empirical Near-Source Attenuation Relationship for Horizontal and Vertical Components of Peak Ground Acceleration Peak Ground Velocity and Pseudo-absolute Acceleration Response Spectra", Seismological Research Letter, **68**(1), 154 p.

40. Boore, D.M. and Joyner (1991). "Estimation of Ground Motion at Deep Soil Sites in Eastern North America", *Bulletin of the Seismological Society of America,* **81**, 2167-2185.

41. Boore, D.M. and Joyner (1997). "Site Amplification for Generic Rock Sites", *Bulletin of the Seismological Society of America,* **87**, 327-34.

42. Campbell, K.W. (2003). "Engineering Models of Strong Ground Motion", In Earthquake Engineering Hand Book, Ed: Chen W. and Scawthorn. **5**, 1-79. CRC Press.

43. Fukushima, Y., Irikura, K., Uetake, T., and Matsumoto, H. (2000). "Characteristics of Observed Peak Amplitude for Strong Motion from the 1995 Hyogoken Nanbu (Kobe) Earthquake", *Bulletin of the Seismological Society of America*, **90**(3), 545-565.

44. National Earthquake Information Center, USGS. (2003). http://earthquake.usgs.gov/.

45. Nowroozi, A.A. and Mohajer-Ashjai, A. (1985). "Fault Movements and Tectonics of Eastern Iran: Boundaries of the Lut Plate", *Geophysical J. Royal Astronomical Society*, **83**, 215-237.

46. Nowroozi, A.A. (1985). "Empirical Relations between Magnitudes and Fault Parameters for Earthquakes in Iran", *Bulletin of the Seismological Society of America*, **75**(5), 1327-1338.

47. Tatar, M., Hatzfeld, D., Moradi, A.S., Paul, A. Farahbod, A.M., and Mokhtari, M. (2004). "Aftershocks Study of the 26 December 2003 Bam Earthquake", *JSEE Special Issue on Bam Earth quake*, pp. 23-31.

48. Harvard Seismology: CMT Search Results (2004). http://www.seismology.harvard.edu/cgi-bin/ CMT2/.

49. Mostafazadeh, M., Farahbod, A.M., Mokhtari, M., and Allamzadeh, M. (2004). "Seismological Aspect of 26 December 2003 Bam Earthquake", *JSEE Special Issue on Bam Earthquake.* pp. 15-21.

50. Zare, M. (2003). "Seismological Aspects of the Bam Earthquake of 26 December 2003, Mw=6.5", IIEES Website, www.iiees.ac.ir.

Appendix 1

Dates, accelerograms codes, and other seismic parameters used for analysis and derivation of coefficients in the acceleration attenuation relationships.

Date	Code	Site	Ms	mb	ML	Mw	Depth	EPD	HYPD	MACD	H1	VER	H2
3/7/75	1006-1	2	6.1	5.9			27	28	48	28	79	39.5	184
3/7/75	1006-2	2	5.11	5.2				28	40	28	17	13	27
3/7/75	1007	1	6.1	5.9			27	71	80	71	18.5	11.5	17.3
3/7/75	1008	1	6.1	5.9			27	50	56	50	15	14.2	14.2
10/8/75	1014-4	3	5.4	5.3			51	32			77	52	82
11/7/76	1043	1	6.4	5.8			13	15	10	14	115	170	157
11/7/76	1047-8	2	6.4	5.8			13	2		2	490	115	550
11/24/76	1046-1	2	7.3	6.1			36	48		61	87	40	82
11/24/76	1046-2	2	5.5	5.5			33	47			68	18	49
3/21/77	1050-1	2	7	6.2			29	46	52	42	115	41	137
3/21/77	1052	1	7	6.2			29	71		70	29	15	21
4/6/77	1054-1	1	6.1	5.6			43	7		2	720	520	615
4/6/77	1055	1	6.1	5.6			33	32		36	18	10.1	18.5
4/6/77	1058	2	6.1	5.6			33	18		22	101	57	83
4/6/77	1059	4	6.1	5.6			33	21		10	88	46.5	64
9/16/78	1082-1	1	7.3	6.7		7.4	10	36	28	20	309	176	377
9/16/78	1083-1	1	7.3	6.7		7.4	10	64	64	45	98	87	94
9/16/78	1084-1	1	7.3	6.7		7.4	10	27	28	5	1103	848	841
9/16/78	1086	3	7.3	6.7		7.4	10	181	140	144	90	22	58
9/16/78	1090-2	3	7.3	6.7		7.4	10	234		220	35	24	44.5
11/4/78	1098-3	3	6	6.2			34	14	20		56	28	58
12/14/78	1096-1	1	6.1	5.9			33		5		74	83	83
1/16/79	1102	3	6.6	6			33	135		140	39	16	31
1/16/79	1106	3	6.6	6			33	66	80	75	32	37	34
1/16/79	1107	1	6.6	6			33	61		65	16	12.5	26
1/16/79	1109	4	6.6	6			33	66	64	85	18	19.5	32.5
1/16/79	1113	2	6.6	6			33	94	80	90	69	30	69
11/14/79	1117	3	6.6	6			33	79	96	80	28	12.5	21
11/14/79	1118	1	6.6	6			33	55		60	36	29.5	45
11/14/79	1121	2	6.6	6			33	79	72	50	100	41	61
11/14/79	1124	1	6.6	6			33	116		105	21	13.5	14.7
11/14/79	1132-2	3	6.6	6			33	184		170	19	10	20
11/14/79	1132-1	1	6.6	6			33	143	132	150	16	14	22.5
11/27/79	1131	3	7.1	6.1			10	153	160	130	50	28	42.5

Appendix 1. Continued ...

Date	Code	Site	Ms	mb	ML	Mw	Depth	EPD	HYPD	MACD	H1	VER	H2
11/27/79	1134-2	3	7.1	6.1			10	152		120	111	37	90
11/27/79	1135	1	7.1	6.1			10	98	88	60	49	29.5	33
11/27/79	1137	1	7.1	6.1			10	127	138	130	29	12.5	22
11/27/79	1138-1	3	7.1	6.1			10	83	80	75	67	39	81
11/27/79	1139	1	7.1	6.1			10	55	44	40	228	136	132
11/27/79	1140-1	1	7.1	6.1			10	83	80	65	69	58.5	80
11/27/79	1141-1	4	7.1	6.1			10	128	120	105	76	35.5	70.5
11/27/79	1142-1	4	7.1	6.1			10	103	92	60	81	61	86
11/27/79	1143-2	2	7.1	6.1			10	75	64	65	145	88	146
11/27/79	1144-2	1	7.1	6.1			10	75	108	105	40.5	41.3	52.5
11/27/79	1145	1	7.1	6.1			10	173	160	165	46	20.3	36
1/12/80	1136-3	1	5.9	5.4			33	26			162	47	271
12/19/80	1153-1	1	5.8	5.6			33	62			13	10.5	10.7
6/11/81	1168	4	6.7	6.1			33	72		85	36.5	19.5	28
6/11/81	1169	1	6.7	6.1			33	43	40	40	25	37	37
6/11/81	1172-6	3	6.7	6.1			33	33	20	1	45	33	62
6/11/81	1179	1	6.7	6.1			33	114		145	33	21	22
7/28/81	1174	4	7.1	5.7			11	55	48	55	91	69	108
7/28/81	1176-5	3	7.1	5.7			11	12		20	198	204	218
7/22/83	1211-1	1	5	5.6			41	16	20	18	28.5	40	36.5
2/2/85	1240-6	3	5.3	5.2	5.6		37	25	7	5	185	79	185
7/12/86	1291-1	2	5.6	5.7			10	45		40	39	132.5	31
12/20/86	1289-5	3	5	5.5			26	20	24		34	15.5	14.5
6/20/90	1351	1	7.7	6.8		7.3	19	210		189	10.3	27	11
6/20/90	1352	1	7.7	6.8		7.3	19	209		189	26	15	19.5
6/20/90	1353	3	7.7	6.8		7.3	19	54	76	52	186	90	134
6/20/90	1354	4	7.7	6.8		7.3	19	91	80	69	149	75	232
6/20/90	1355	4	7.7	6.8		7.3	19	89	68	70	102	69	83
6/20/90	1357-1	4	7.7	6.8		7.3	19	97	96	61	108	75	176
6/20/90	1359	4	7.7	6.8		7.3	19	131	100	105	115	26.5	72
6/20/90	1360	2	7.7	6.8		7.3	19	9	12	1	538	184	418
6/20/90	1361	3	7.7	6.8		7.3	19	185	176	170	16.5	30.5	19.5
6/20/90	1362-1	1	7.7	6.8		7.3	19	43	40	8	526	548	503
6/20/90	1363-1	4	7.7	6.8		7.3	19	224		202	46	28	35
6/20/90	1364	1	7.7	6.8		7.3	19	75	80	57	125	51	60
6/20/90	1365	4	7.7	6.8		7.3	19	195		160	30	15	29
6/20/90	1366	1	7.7	6.8		7.3	19	212		189	13	18.4	13.3
6/20/90	1369	4	7.7	6.8		7.3	10	198		185	40	32	44
6/20/90	1370-2	1	7.7	6.8		7.3	10	207		185	13	19	17
6/20/90	1371-2	1	7.7	6.8		7.3	10	177		151	35	13	12
6/20/90	1372	4	7.7	6.8		7.3	10	143	140	122	72	44	77
7/6/90	1382-1	3	5.2	4.5			51	16			48.5	18.3	38.5
11/28/91	1420-2	3	5	5.6	5.5		16	26		14	61	16.3	63.2
3/8/94	1491	2	6.3		5.7				12	36	42	19	26
3/30/94	1492-6	1	5.6	5.5		5.4	54	17	24		213	61	245
6/20/94	1492-16	1	5.7	5.9		5.9	9	29		29	306	104	257
6/20/94	1493-2	3	5.7	5.9		5.9	9	17		17	244	116	282
6/20/94	1495	1	5.7	5.9		5.9	9	50		50	21	12	19

Appendix 1. Continued ...

Date	Code	Site	Ms	mb	ML	Mw	Depth	EPD	HYPD	MACD	H1	VER	H2
6/20/94	1498	2	5.7	5.9		5.9	9	63		63	28	15	29
6/20/94	1502-9	2	5.7	5.9		5.9	9	7		7	1057	993	1070
7/31/94	1506-1	4	5.3	5.3		5.6	43	20	22		187	129	103
7/31/94	1525	1	5.3	5.3		5.6	43	26			13	15	13
7/31/94	1526-1	1	5.3	5.3		5.6	43	11	18		26	26	22
7/31/94	1526-2	1	5.11	5.2			73	8	17		4.6	10	7.2
7/31/94	1527	1	5.3	5.3		5.6	43	7	35		28	29	26
9/20/94	1508-2	1	5.4		4.9		33		19	15	17	20	36
1/24/95	1528-3	3	5.1	4.9		5	33	22	8	5	545	416	496

EPD, HYPD and MACD are epicentral, hypocentral and macroseismic distance in km respectively.

H1, H2 and VER are horizontal 1, horizontal 2 and vertical component of accelerations in cm/s.s.

Table is modified from Bard et al [7].